Microporous Activated Carbon Spheres Prepared from Resole-Type Crosslinked Phenolic Beads by Physical Activation

Arjun Singh,[1] Darshan Lal[2]

[1]*Terminal Ballistic Research Laboratory, Ministry of Defence, Sector 30, Chandigarh (Union Territory) 160020, India*
[2]*Defence Materials and Stores Research and Development Establishment, Post Office, Grand Trunk Road, Kanpur 208013, India*

Received 13 October 2007; accepted 26 May 2008
DOI 10.1002/app.28846
Published online 10 September 2008 in Wiley InterScience (www.interscience.wiley.com).

ABSTRACT: Microporous activated carbon spheres (ACSs) with a high specific Brunauer–Emmet–Teller (BET) surface area were prepared from resole-type spherical crosslinked phenolic beads (PBs) by physical activation. The PBs used as precursors were synthesized in our laboratory through the mixing of phenol and formaldehyde in the presence of an alkaline medium by suspension polymerization. The effects of the gasification time, temperature, and flow rate of the gasifying agent on the surface properties of ACSs were investigated. ACSs with a controllable pore structure derived from carbonized PBs were prepared by CO_2 gasification. Surface properties of ACSs, such as the BET surface area, pore volume, pore size distribution, and pore diameters, were characterized with BET and Dubinin–Reduchkevich equations based on N_2 adsorption isotherms at 77 K. The results showed that ACSs with a 32–88% extent of burn-off with CO_2 gasification exhibited a BET surface area ranging from 574 to 3101 m^2/g, with the pore volume significantly increased from 0.29 to 2.08 cm^3/g. The pore size and its distribution could be tailored by the selection of suitable conditions, including the gasification time, temperature, and flow rate of the gasifying agents. The experimental results of this analysis revealed that ACSs obtained under different conditions were mainly microporous. The development of the surface morphology of ACSs was also studied with scanning electron microscopy. © 2008 Wiley Periodicals, Inc. J Appl Polym Sci 110: 3283–3291, 2008

Key words: adsorption; microstructure; morphology; resins

INTRODUCTION

In general, activated carbons in both powdered and granular forms are widely used as adsorbents because of their excellent adsorption capability for the removal of toxic agents.[1,2] The applicability of these carbons mainly depends on the specific surface area and pore structure properties. The type of porosity developing in activated carbons is strongly dependent on the starting precursor materials, activation methods, and processing parameter conditions.[3]

These activated carbons are generally produced by physical activation or chemical activation methods.[4] Physical activation is performed in two steps: carbonization of the raw materials followed by gasification in the presence of some oxidizing agents, such as steam, oxygen, and carbon dioxide.[5] On the other hand, the chemical activation process is performed through the thermal decomposition of precursor materials impregnated with dehydrating agents, such as potassium hydroxide, zinc chloride, and phosphoric acid.[6–8] In this activation, all chemicals act as hydrating agents.

The activated carbons are prepared from both natural and polymeric precursor materials with both physical and chemical activation methods. Polymeric precursor materials have an advantage over natural ones, in that they produce activated carbons with high surface areas and desired pore structures.[9] In general, polymeric precursor materials used to produce activated carbons are polyacrylonitrile, polystyrene sulfonate and its derivatives, poly(vinyl chloride), divinylbenzene and its copolymers, polystyrene divinyl, and phenolic resins.[10–18] Moreover, because of their low level of inorganic impurities and negligible ash content, phenolic resins are promising polymeric precursor materials for producing high surface areas and desired pore structures, which can be controlled to very low levels in the synthesis process.[10,11] They are easy to prepare in desired physical forms (powders, granules, and fibers).[19,20]

Recently, activated carbons in spherical forms have been prepared from different precursor materials, such as pitch, polyacrylonitrile, polystyrene

Correspondence to: A. Singh (arjunsngh@yahoo.com).

sulfonate resins, and phenolic resins. They have exhibited better abrasion resistance because of the absence of sharp edges and irregular shapes in comparison with conventional activated carbon powder. Advanced adsorbent materials, namely, activated carbon spheres (ACSs), have been developed that are highly effective in a spherical form when adhered to a base fabric for protection against chemical warfare agents. Microporous ACSs prepared from divinylbenzene are used for protection against chemical warfare agents.[21] They are also outstanding materials used for the purification of gases and water.

Yang and coworkers[22,23] reported the preparation of ACSs by the addition of pore-forming agents such as poly(ethylene glycol), poly(vinyl butyral), and ferrocene to a novolac-type resin. The ACSs prepared with the aforementioned precursors by steam activation showed more mesopores with a low product yield. They further attempted to prepare ACSs from a novolac-type phenolic resin by supercritical water activation. The ACSs prepared by this method showed cracks on the surface with a low surface area (919 m^2/g) and lost their mechanical strength. Therefore, today's requirement is to develop a polymeric precursor material that produces ACSs with a controlled pore structure and a high adsorption capacity with sufficient mechanical strength.

Here we synthesized resole-type spherical phenolic beads (PBs) as precursor materials by a polymerization technique.[24] ACSs from resole-type crosslinked spherical PBs have not yet been reported in the literature. Apart from the activation conditions, it has been reported that the structure of the precursor materials also has an effect on the resulting activated carbons. When a phenolic resin is used as a precursor material, the structure and mechanical properties[25] depend on the molar ratios of the phenol and formaldehyde as well as the concentration of the catalyst, synthetic temperature, and curing time. Furthermore, we optimized these parameters and used precursor materials that produced ACSs with higher surface properties and better mechanical strength.

This work describes the preparation of microporous ACSs with higher specific Brunauer–Emmet–Teller (BET) surface areas from carbonized PBs by CO_2 gasification. The surface properties under study include the specific BET surface area, pore volume, micropore volume, and pore size distribution. The effects of process parameters such as the gasification time, temperature, and flow rate of CO_2 on the surface properties were investigated. The surface morphology of ACSs was also studied with scanning electron microscopy (SEM) and is discussed.

EXPERIMENTAL

Materials

Phenol (Chemical Division, Ranbaxy Laboratories, Ltd., Mumbai, India), an aqueous formaldehyde solution (37–41% w/v, Laboratory-reagent; S.D. Fine Chemical, Ltd., Mumbai, India), poly(vinyl alcohol) (weight-average molecular weight = 125,000; S.D. Fine Chemical, Mumbai, India), triethylamine (99%; Lancaster Synthesis, Morecaube, England), LR hexamine (hexamethylene tetraamine; S.D. Fine Chemical), and analytical-reagent acetone (Samir Tech-Chem Pvt., Ltd., Gurgaon, India) were used as received.

Preparation of the precursor material

The process for the preparation of PBs is described in our previous article.[24] In this process, the reaction was carried out in a 1000-mL, round-bottom, four-neck reaction vessel with a Teflon stirrer, a reflux condenser, and a thermocouple. The phenol was polymerized with an aqueous solution of formaldehyde in a molar ratio of 1 : 1.5 in the presence of the initiator triethylamine (1.5 wt %), and this was followed by dispersion in the resulting mixture in distilled water (25.0 wt %) with the help of a stirrer via stirring at 550 rpm. The reactor was charged with this mixture along with an aqueous solution of poly (vinyl alcohol) (5.0 wt %) as a stabilizer at 96 ± 1°C for 40 min. Then, hexamethylene tetraamine (5.5 wt %) was added to the reaction vessel, and the polymerization was carried out at the same temperature and fixed agitation rate (550 rpm) for 4 h. At the end of the reaction, the reactor was cooled, and the beads were separated from the reaction mixture by filtration and washed with water. Finally, they were washed with acetone and dried to get the PBs.

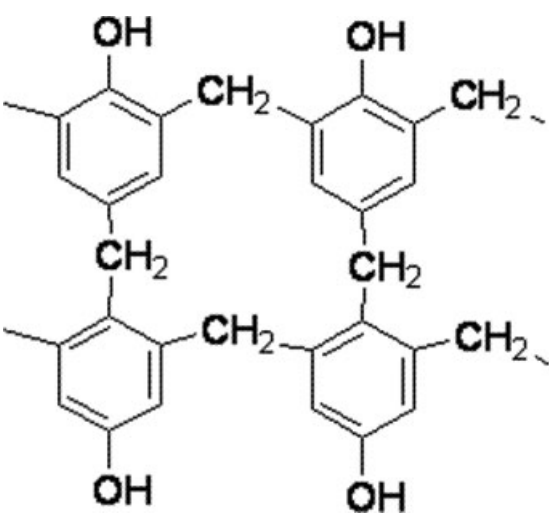

Scheme 1 Illustration of the structure of the cured resole-type phenolic resin.

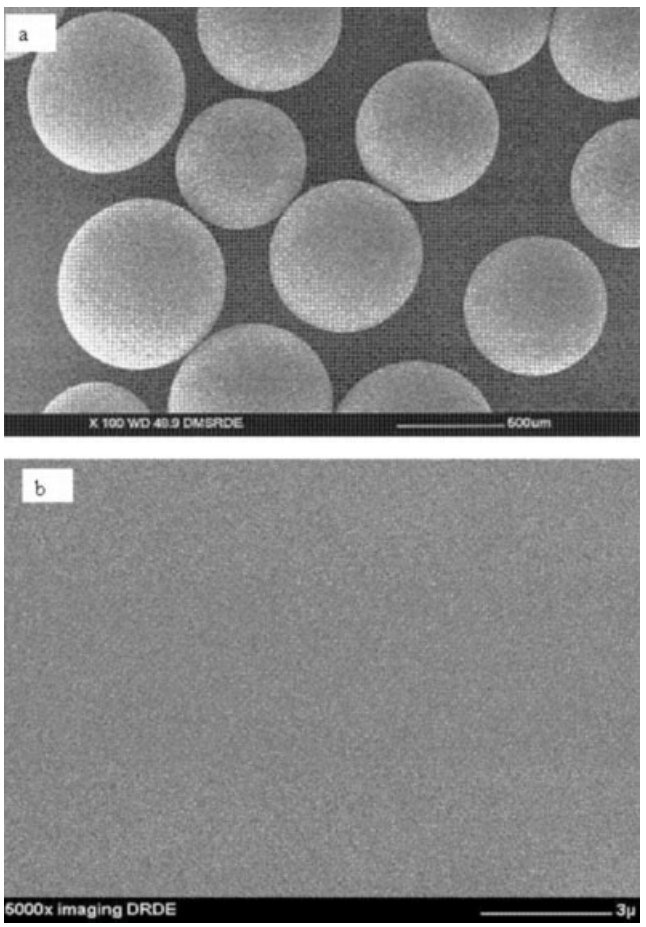

Figure 1 SEM photographs of (a) PBs and (b) the internal surface of PBs.

The phenol and formaldehyde under alkaline conditions and, therefore, the formation of the cross-linked PB structure with *ortho*- and *para*-methylene bridges between rings are shown in Scheme 1. Most studies have revealed that the concentration of ether bridges can be negligible.

Preparation of ACSs

ACSs were prepared by the carbonization of PBs in an N_2 atmosphere followed by CO_2 gasification. PBs with a particle size distribution of 0.2–1.0 mm were carbonized in a vertical tubular furnace at a heating rate of 5°C/min from room temperature to the highest treatment temperature of 800°C. The carbonized material was further activated in the same tubular furnace reactor by CO_2 gasification. The experimental sets of ACS samples at different gasification times (5–15 h), temperatures (850–1150°C), and flow rates (0.25–1.0 L/min) were obtained as follows. Samples ACS_{32}, ACS_{53}, ACS_{67}, and ACS_{88} were prepared with different extents of burn-off (32, 53, 67, and 88%, respectively) at 950°C; samples ACS_{850}, ACS_{950}, ACS_{1050}, and ACS_{1150} were prepared at different temperatures (850, 950, 1050, and 1150°C, respectively) for 5 h; and samples $ACS_{0.25}$, $ACS_{0.5}$, $ACS_{0.75}$, and $ACS_{1.0}$ were prepared at different flow rates (0.25, 0.5, 0.75, and 1.0 L/min, respectively) at 950°C for 5 h.

Characterization methods

The particle size distribution of PBs was measured with mesh sieves of various sizes. The specific BET surface areas and pore structure parameters of ACSs were determined from the adsorption isotherm of a nitrogen molecule at 77 K with a Quantachrome Autosorb (Quantachrome Instruments, FL). The BET equation was used to calculate the surface area.[26] Before the measurement of the specific BET surface areas and pore structure parameters, the samples were outgassed at 250°C in a vacuum oven for 4 h. The micropore volume of the ACSs was determined with the Dubinin–Reduchkevich (DR) equation.[27] The total pore volume was obtained from the amount of nitrogen adsorbed at a relative pressure of 0.95 to the liquid nitrogen volume.[28] The subtraction of the micropore volume (from the DR equation) from the total pore volume gave the mesopore volume.[29]

The mechanical strength of ACSs was obtained with a carbon and sphere tester (ASTM C-695 and ASTM E-4). For more accuracy in the results, 10 spheres were taken from each sample (ACS_{850}, ACS_{950}, ACS_{1050}, and ACS_{1150}), and the average value corresponding to the mechanical strength of the ACSs was taken. The surface morphology of the beads was studied with a JEOL scanning electron microscope (Tokyo, Japan). The samples were sputter-coated with gold before analysis. Elemental analysis was carried out with a Carlo-Erba elemental analyzer (Germany). The average pore size (or pore diameter) of ACSs was calculated from 4 times the total pore volume (cm^3/g) over the corresponding specific BET surface area (m^2/g), and it was assumed that the pores were cylindrical. The yield percentage of ACSs was calculated from the mass of the resulting activated carbons divided by the mass of the raw material.

RESULTS AND DISCUSSION

Starting material

The SEM image in Figure 1(a) shows that the PBs prepared from phenol and formaldehyde in a basic

TABLE I
Elemental and Proximate Analyses of PBs

Elemental analysis (wt %)		Proximate analysis (wt %)	
Carbon	68.9	Moisture	0.3
Nitrogen	1.5	Volatile matter	35.1
Hydrogen	6.3	Fixed carbon	64.6
Oxygen	23.3	Ash	0.0

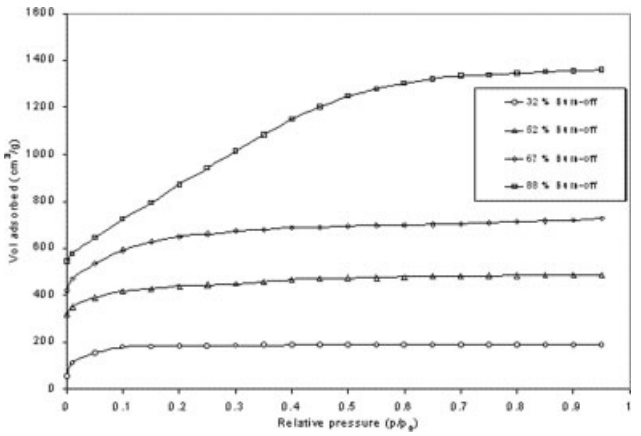

Figure 2 Adsorption isotherms of N_2 at 77 K on ACSs prepared from PBs at 950°C to different extents of burn-off.

catalyst were spherical in shape and had a smooth surface. The SEM image in Figure 1(b) at a higher magnification shows that no pores were found on the external surface of these beads, and this confirms the absence of macropores.

Table I shows the elemental and proximate analyses of PBs, which are reported on a dry-ash-free basis and dry basis, respectively. In the elemental analyses, PBs were dried at 100°C in a vacuum oven for 2 h, and the oxygen content was obtained from the difference. The elemental analyses show that the PBs had carbon, hydrogen, oxygen, and nitrogen contents of 68.9, 6.3, 23.3, and 1.5, respectively. As can be seen in Table I, the PBs had nitrogen contents (1.5) indicating the incorporation of nitrogen into the PBs from hexamine during the polymerization reaction. In dry-basis analyses, ash and volatile matter contents of the PBs were calculated on a moisture-free basis. The proximate analyses of the PBs showed that the moisture, ash, and volatile matter contents were 0.3, 0.0, and 35.1%, respectively. The proximate analyses clearly indicated that the PBs had 64.6% fixed carbon and were free from ash content.

Effect of the gasification time

Figure 2 shows adsorption isotherms of N_2 of the ACSs prepared with different gasification times (extents of burn-off). The adsorption isotherms of ACSs at 32, 53, and 62% burn-off were mainly type I isotherms, in which the knees of the isotherms at a low relative pressure (0.1) were sharp and plateaus were fairy horizontal. It is clear that N_2 adsorption on ACS_{32}, ACS_{53}, and ACS_{67} led to type I isotherms. However, the N_2 adsorption isotherm of ACS_{88} at 88% burn-off significantly differed from that at 32, 53, and 67% burn-off. Figure 2 shows that ACS_{88} at 88% burn-off exhibited a more significant increase in adsorption at a higher relative pressure, and this indicates that the isotherm of sample ACS_{88} was a mixture of type I and type IV. This also indicates that sample ACS_{88} showed both a microporous and mesoporous nature according to Brunauer, Deming, Deming and Teller (BDDT) classification.[30] The data derived from adsorption isotherms of ACSs in Figure 2 are listed in Table II.

Table II summarizes the activation conditions, yields, N_2 BET surface areas, pore volumes, micropore volumes, and average pore diameters of the prepared ACSs. The results show that the gasification time is a very important parameter in developing the pore structure of ACSs from PBs. Table II shows that the surface properties, including the BET surface area, pore volume, and average pore diameter, monotonically increased with the extent of burn-off with CO_2 gasification. The results agree with those reported earlier for ACSs prepared from divinyl benzene and a novolac-type resin.[21,30] The prepared ACSs exhibited a BET surface area ranging from 574 to 3101 m^2/g with extents of burn-off of 32–88%. The maximum BET surface area value of 3101 m^2/g is the largest for available ACSs[21,23,29,30] according to the literature.

Table II shows that the pore volume increased, ranging from 0.29 to 2.08 cm^3/g, with the burn-off increasing from 32 to 88%. The pore volume values of ACSs from PBs were much higher than those of ACSs prepared from various polymeric precursor

TABLE II
Effect of the Gasification Time on the Surface Characteristics of ACSs from PBs with Physical Activation[a]

Sample code	Char burn-off (%)	Yield (%)	Specific BET surface area (m^2/g)	Total pore volume (cm^3/g)	Pore size distribution		Average pore diameter (Å)
					Micropore volume (%)	Mesopore volume (%)	
ACS_{32}	32	44.2	574	0.29	97.1	2.9	20.2
ACS_{53}	53	30.6	1390	0.73	94.8	5.2	21.0
ACS_{67}	67	21.4	2082	1.12	91.1	8.9	21.5
ACS_{88}	88	7.5	3101	2.08	67.4	32.6	26.8

[a] The activation was carried out at 950°C under the CO_2 gasifying agent for different degrees of burn-off.

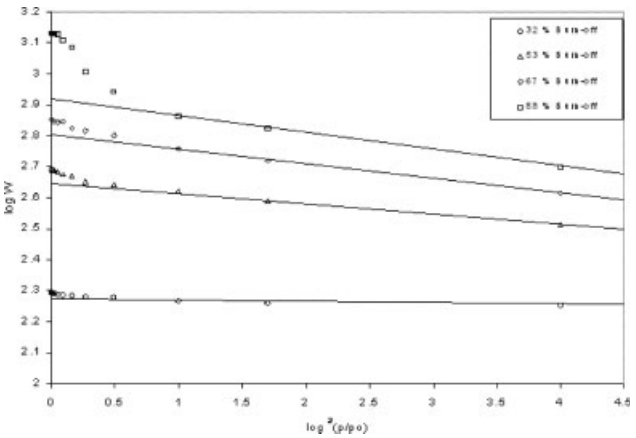

Figure 3 DR plots of ACSs prepared from PBs at 950°C to various degrees of burn-off.

materials mentioned in other studies.[21,23,29] The yield of ACSs during activation clearly decreased with an increase in the extent of burn-off.

For the assessment of microporosity, the DR equation[31] was used:

$$W = W_o \exp\{-[RT \log(p_o/p)/\beta E_0]^2\} \quad (1)$$

where W is the volume filled at temperature T and relative pressure p_o/p, W_o is the total volume of the micropores, E_0 is the characteristic adsorption energy for the standard, β is the adsorbate affinity coefficient (taken to be 0.34 for nitrogen), and R is the gas constant.

Figure 3 shows the DR plots of log W versus $\log^2(p_o/p)$. The ACSs produced linear DR plots over a wide range of relative pressures, which indicated a narrow pore size distribution. The upward deviation points from linear DR plots at high values of the relative pressure indicated the presence of mesopores. The upward deviation curve from linear DR plots increased with the extent of burn-off, and this indicated an excess of mesoporosity. Table II shows that the micropore volume of ACSs decreased from 97.1 to 67.4% when the extent of burn-off increased from 32 to 88%. These results indicate that the extent of burn-off with CO_2 gasification promoted the formation of mesopores.

Basically, the type of porosity developed in activated carbons depends on the type of precursor material employed and the activation methods, which can affect the final pore size distribution.[32] Teng and Wang[33] prepared activated carbons with a specific BET surface area up to 2220 m^2/g at a higher burn-off of 78% and with a carbon yield of 12.0% by a physical and chemical etching method from phenol–formaldehyde resins, which were grounded and sieved. Lin and Teng[34] reported that cured resins carbonized in N_2 at 700°C, and this was followed by gasification of the resulting char in steam at the same temperature for different extents of burn-off. The activated carbons showed a high BET surface area (2100 m^2/g) at higher burn-off levels (~ 80%), which corresponded to a low carbon yield (<10%). Furthermore, activated carbon from urea-impregnated cured resins[34] under the same conditions reported previously showed a higher BET surface area of 2000 m^2/g at 70% burn-off.

Activated carbons prepared in a spherical form have an advantage over powder ones, in that they have better abrasion resistance due to the absence of sharp edges and irregular shapes. Yang et al.[23] prepared ACSs from a novolac-type phenolic resin with a pore-forming agent. When the precursor was activated to a high degree of burn-off of 62%, they obtained a BET surface area of 1663 m^2/g and a mesoporosity of 37%. Cai et al.[40] also attempted to prepare ACSs from a novolac-type phenolic resin as a precursor by supercritical water activation. The prepared ACSs from supercritical water activation, which had a degree of carbon burn-off of 50.8%, possessed a BET surface area of 919 m^2/g and a mesoporosity of 17.0%.

In contrast, we prepared resole-type cured spherical PBs as precursors from phenol and formaldehyde by a suspension polymerization technique. Table II shows that the prepared ACSs from PBs had a BET surface area of 1390 m^2/g with a mesoporosity of 5.2% at a degree of burn-off of 53.0%. The material was further activated to a higher extent of burn-off of 88.0%. The ACSs showed a specific BET surface area greater than 3100 m^2/g and a mesoporosity of 32.6%. This indicated that the ACSs were gasified with CO_2 inside the beads, and the outer shape of the particles remained more or less unchanged. Therefore, the porosity of the ACSs was increased linearly with the extent of burn-off. The results showed that the ACSs prepared from resole-type PBs as precursors by CO_2 gasification had predominantly a microstructure with higher surface properties.

Effect of the gasification temperature

The ACSs prepared from PBs at different temperatures (850–1150°C) for 5 h via physical activation[36,37] with CO_2 were investigated by N_2 adsorption. Figure 4 shows that the isotherms are typical of microporous carbons because the knees of the adsorption isotherms are sharp with horizontal plateaus. The data show that the amount of volume adsorbed at a specific relative pressure increased with the gasification temperature increasing and reached a maximum at 1150°C. Above 1050°C, the N_2 adsorption capacity increased with increasing temperature, but the volume adsorbed at a higher relative pressure at

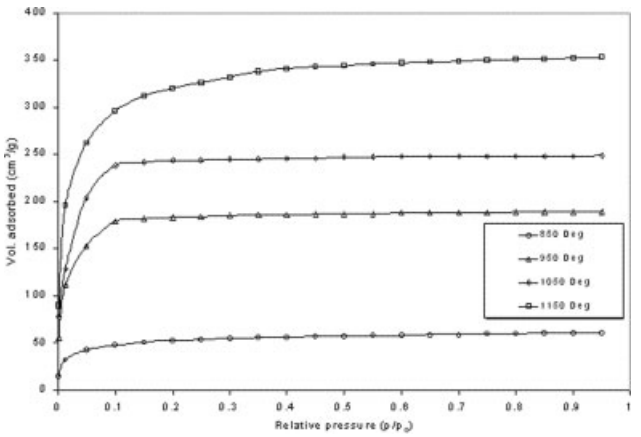

Figure 4 Adsorption isotherms of N_2 on ACSs prepared from PBs at different temperatures (850–1150°C) for 5 h.

1150°C indicated a widening of pores with the gasification temperature increasing. The development of porosity at 1150°C may have been due to increased reactivity of CO_2, which caused the breakdown of the carbon matrix. Figure 4 shows that the adsorption isotherms of ACSs changed the maximum between gasification temperatures of 850 and 950°C, whereas there was a small amount of N_2 adsorbed at 850°C. This indicated that the porosity developed at temperatures higher than 850°C.

Table III shows the results for the surface properties of ACSs obtained from adsorption isotherms of N_2. The yield percentage of ACSs decreased as the gasification temperature increased. At a higher temperature, the activation of char became more extensive, and this resulted in a low yield and widening of the pore structure.

As for the variation of the surface properties with the activation conditions, Table III shows that the specific BET surface area and pore volume increased with the gasification temperature increasing. The increase in the porosity with the gasification temperature could be attributed to enhanced carbon gasification and space that was previously occupied by the decomposed materials.[38] ACSs prepared at 1050°C had a BET surface area of 746 m^2/g with a micropore structure. Although the BET surface area increased at a high temperature (1150°C), the ACS matrix broke down. This could be attributed to the thermal treatment, which caused the breakdown of crosslinks in the carbon matrix. Because of the breakdown of the carbon matrix, there was significant development of mesoporosity of 11.3%. It is also possible that the extensive gasification at high temperatures resulted in the destruction of pore structures.[36]

Effect of the flow rate of the gasifying agent (CO_2)

With respect to the gasification time and temperature, the flow rate of the gasifying agent plays an important role in the development of porosity in activated carbons. Generally, the slower the reaction is, the more extensive the development of porosity is within the particle (e.g., the gasifying agents must penetrate the particles to remove carbon atoms and create pores). Adsorption isotherms of N_2 on ACSs at 950°C for 5 h at different flow rates are shown in Figure 5.

Figure 5 shows that the N_2 adsorption isotherms of samples $ACS_{0.25}$, $ACS_{0.5}$, and $ACS_{0.75}$ present typical microporosity, which corresponds to type I of the IUPAC classification, whereas the adsorption isotherm for sample $ACS_{1.0}$ is a mixture of type I and type IV, reflecting microporous and mesoporous natures according to the BDDT classification.[31] The adsorption isotherms of the ACSs showed a maximum change in the volume adsorbed when the flow rate of CO_2 varied from 0.25 to 0.5 L/min. At a low flow rate of 0.25 L/min, the opening of the knee of the isotherms and the volume adsorbed increased with the relative pressure, and this indicated a widening of the porosity. The significant development of porosity at a low flow rate of CO_2 was due to increased contact time between the beads and CO_2, which easily diffused inside the beads; this was followed by CO_2 gasification.

Table IV shows the surface properties of ACSs derived from adsorption isotherms of N_2 in Figure 5.

TABLE III
Effect of the Gasification Temperature on the Surface Characteristics of ACSs from PBs with Physical Activation[a]

Sample code	Gasification temperature (°C)	Yield (%)	Specific BET surface area (m^2/g)	Total pore volume (cm^3/g)	Pore size distribution		Average pore diameter (Å)
					Micropore volume (%)	Mesopore volume (%)	
ACS_{850}	850	59.9	162	0.088	90.9	9.1	21.7
ACS_{950}	950	44.2	574	0.291	97.1	2.9	20.2
ACS_{1050}	1050	36.5	746	0.385	99.1	0.9	20.6
ACS_{1150}	1150	23.5	1031	0.546	88.7	11.3	21.2

[a] The activation was carried out by PBs with the gasifying agent CO_2 at different gasification temperatures and was then maintained at the same temperature for 5 h.

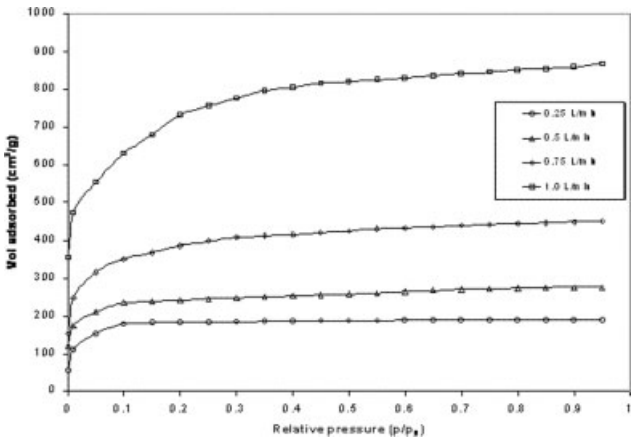

Figure 5 Adsorption isotherms of N_2 on ACSs prepared at different flow rates (0.25–1.0 L/min).

Both the BET surface area and mesoporosity increased with the flow rate of CO_2 decreasing. At a low flow rate of CO_2, the ACSs exhibited a BET surface area of 2482 m^2/g with 10.9% mesoporosity. This indicated that the gasifying agent (CO_2) penetrated the beads and removed carbon atoms; this enhanced the surface area and pore volume in the carbons.[39] However, at a high flow rate (1.0 L/min), the porosity of the ACSs was found to be low (574 m^2/g), and this was due to less diffusion of CO_2 inside the carbonized beads.

Because of the gasification mechanism, the yield of ACSs decreased with a decreased flow rate of the gasifying agent, as shown in Table IV. At a low flow rate of 0.25 L/min, the $ACS_{0.25}$ yield was 10.8% for a gasification time of 5 h. This indicated that the rate of reaction with CO_2 gasification was very fast and produced a high BET surface area, which is considered an important issue in physical activation.

Mechanical strength of ACSs

Figure 6 shows the mechanical strength of ACSs prepared at 950°C with different extents of burn-off. The mechanical strength of the ACSs decreased with the extent of burn-off. The strength of the ACSs decreased from 120 to 3 N/mm^2 when the extent of burn-off increased from 32 to 88%. There was maximum loss of mechanical strength of ACSs at higher burn-off. The sample ACS_{53}, prepared from resole-type PBs at 950°C with 53% burn-off, exhibited a high surface area of 1390 m^2/g with excellent mechanical strength in comparison with reported ACSs.[21,23,29,40] In contrast, the ACSs prepared from a novolac-type phenolic resin by steam activation[23,40] showed cracks on the surface at low extents of burn-off, and they lost their mechanical strength with a low surface area (<950 m^2/g).

SEM observation

Figure 7 shows SEM photographs of ACSs prepared at 950°C with different extents of burn-off. The effects of various extents of burn-off can be clearly observed from the SEM images. Figure 7(a,b) shows that ACSs prepared with low extents of burn-off showed no pores on external surfaces at a low magnification. However, Figure 7(c,d) shows that macropores developed on the external surfaces of ACSs prepared with higher extents of burn-off. The porosity on the external surfaces of ACSs significantly increased with the extent of burn-off with CO_2 gasification. Moreover, the ACSs had a smooth surface without any cracks, as found in previous studies.[23,40] The cracking on the external surface of ACSs caused a reduction of the mechanical strength, and this is not promising for developing ACSs for commercial purposes.

The results showed that the gasifying agent CO_2 had strong penetrability and diffusivity through the particles. There was a homogeneous activation reaction between the particles and CO_2, due to which a uniform porous structure was obtained. The carbon reactivity depended on the adsorption, diffusion of the gasifying agent through the solids, and reaction and desorption of gaseous products. Because all the ACSs gasified inside the particles, the outer shape of

TABLE IV
Effect of the Flow Rate of CO_2 as the Gasifying Agent on the Surface Characteristics of ACSs from PBs with Physical Activation[a]

Sample code	Flow rate (L/min)	Yield (%)	Specific BET surface area (m^2/g)	Total pore volume (cm^3/g)	Pore size distribution		Average pore diameter (Å)
					Micropore volume (%)	Mesopore volume (%)	
$ACS_{0.25}$	0.25	10.8	2482	1.34	89.1	10.9	21.6
$ACS_{0.5}$	0.5	23.5	1326	0.69	93.4	6.6	20.8
$ACS_{0.75}$	0.75	36.5	791	0.41	94.3	5.7	20.7
$ACS_{1.0}$	1.0	44.2	574	0.29	97.1	2.9	20.2

[a] The activation was carried out at a gasification temperature of 950°C with different flow rates of CO_2 for 5 h before cooling.

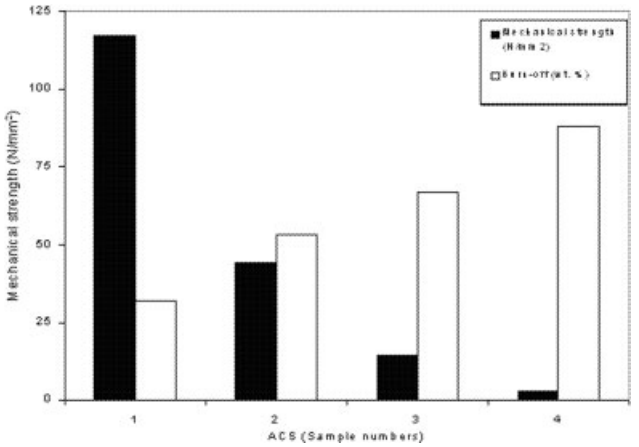

Figure 6 Mechanical strength of ACSs prepared at 950°C and various degrees of burn-off: (1) ACS_{32}, (2) ACS_{53}, (3) ACS_{67}, and (4) ACS_{88}.

the particles remained more or less unchanged. Therefore, the porosity increased linearly with the extent of burn-off, and no cracks appeared on the external surface as a result.

CONCLUSIONS

This study revealed that microporous ACSs with a higher BET surface area could be obtained from resole-type PBs with a physical activation process. We experimentally studied the effects of processing parameters such as the gasification time, temperature, and flow rate. ACSs prepared from PBs at 950°C with CO_2 gasification had increased BET surface areas, mesopore volumes, and pore volumes with the gasification time (the extent of burn-off). The ACSs had a high BET surface area of 3101 m^2/g and a higher pore volume of 2.08 cm^3/g. These ACSs were mainly microporous, and the micropore volume decreased from 97.1 to 67.4% when the extent of burn-off varied from 32 to 88%. The porosity of the ACSs also increased with the temperature increasing from 850 to 1150°C. Finally, an appropriate flow rate was necessity to prepare highly microporous ACSs. In our study, the porosity of the ACSs decreased with the flow rate increasing from 0.25 to 1.0 L/min. ACSs produced at a flow rate of 0.25 mL/min exhibited a BET surface area of 2482 m^2/g with 89.1% microporosity. The SEM

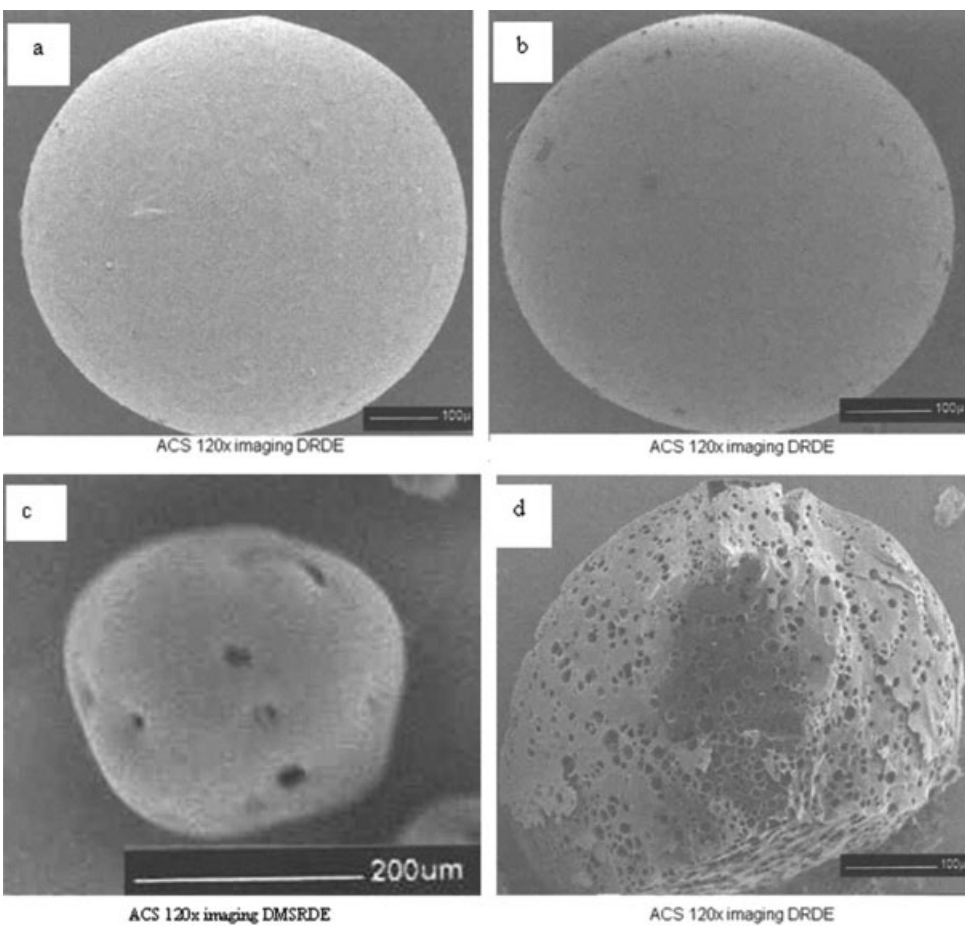

Figure 7 SEM photographs of ACSs prepared at 950°C for (a) 32, (b) 53, (c) 67, and (d) 88% burn-off.

photographs clearly showed that pores developed inside the beads, and no cracks appeared on the external surface. The mechanical strength of the ACSs varied from 120 to 3 N/mm^2 when the extent of burn-off varied from 32 to 88%. Therefore, ACSs prepared from resole-type PBs as precursors by CO_2 activation can show higher surface properties and better mechanical strength.

The authors gratefully acknowledge Beer Singh for his help and R. K. Yadav for the studied BET interpretation. They also thank K. U. B. Rao, Director of the Defence Materials and Stores Research and Development Establishment (Kanpur, India), and M. O. Garg, Director of Indian Institute of Petroleum (DehraDun, India), for their reviews and for much useful advice, which led to improvements to this article. The authors also thank S. A. Ahmad for his full support and cooperation.

References

1. Bansal, R. C.; Donnet, J. B.; Strekli, H. F. Activated Carbon; Marcel Dekker: New York, 1988.
2. El-Geundi, M. S. Adsorption Sci Technol 1977, 15, 777.
3. Linares-Castello, D.; Lillo-Rodenas, M. A.; Cazorla-Amoros, D.; Linarres-Solano, A. Carbon 2001, 39, 741.
4. Introduction to Carbon Technologies: Handbook; Rodriguez-Reinoso, F.; Marsh, H.; Heintz, E. A., Eds.; University of Alicate: Alicate, Spain, 1997; Chapter 2, p 35.
5. Cheremisinoff, P. M.; Ellerbusch, C. Carbon Adsorption Handbook; American Arborist Society: Ann Arbor, MI, 1978.
6. Daley, M. A.; Tandon, D.; Economy, I.; Hippo, E. Ind Eng Chem Res 1996, 34, 1191.
7. Teng, H.; Wang, S. C. Ind Eng Chem Res 2000, 39, 673.
8. Guo, J.; Lua, C. Microporous Mesoporous Mater 1999, 32, 111.
9. Kyobani, T. Carbon 2000, 38, 269.
10. Jain, M. K.; Abhiraman, A. S. J Mater Sci 1987, 22, 278.
11. Jain, M. K.; Balasubramanian, H.; Desai, D. J Mater Sci 1987, 22, 301.
12. Centeno, T. A.; Fuertes, A. B. Carbon 2000, 38, 1067.
13. Tennison, S. R. Appl Catal A 1998, 173, 289.
14. Takecichi, T.; Yamazaki, Y.; Zuo, M.; Ito, A.; Matsumoto, A.; Inagaki, M. Carbon 2000, 39, 257.
15. Lahaye, J.; Nanse, G.; Bagreev-Strelko, V. Carbon 1999, 37, 585.
16. Hu, Z.; Srinivasan, M. P.; Ni, Y. Carbon 2001, 39, 877.
17. Kocirik, M.; Brych, J.; Hradil, J. Carbon 2001, 39, 1919.
18. Tanaike, O.; Fukuoka, M.; Inagaki, M. Synth Met 2002, 125, 255.
19. Amano, I.; Kano, H.; Takahira, H.; Yamamoto, Y.; Itok, K.; Iwatsuki, S. Artificial Kidney, Artificial Liver, and Artificial Cell; Plenum: New York, 1978; pp 89–98.
20. Wilcox, D. L.; Berg, M. Mater Res Symp Proc 1995, 372, 3.
21. Yenisoy-Karakas, S. S.; Aygun, A.; Gunes, M.; Tahtasakal, E. Carbon 2004, 42, 477.
22. Yang, J. B. Ph.D. Thesis, Institute of Coal Chemistry, 1999.
23. Yang, J. B.; Ling, C.; Liu, L.; Kang, F. Y.; Huang, Z. H.; Wu, H. Carbon 2002, 40, 911.
24. Singh, A.; Lal, D. J Appl Polym Sci 2006, 100, 2323.
25. Astarloa, A. G.; Echeverria, J. M.; Martin, M. D.; Mondragon, I. Polymer 2000, 41, 6797.
26. Gregg, S.; Sing, K. S. W. Adsorption, Surface Area and Porosity; Academic: London, 1982; p 42.
27. Gregg, S.; Sing, K. S. W. Adsorption, Surface Area and Porosity; Academic: London, 1982; p 195.
28. Freeman, J. J.; Gimblett, F. G. R.; Sing, K. C. W. Carbon 1989, 27, 7.
29. Singh, G. S.; Lal, D.; Tripathi, V. S. J Chromatogr A 2004, 1036, 189.
30. Brunauer, S.; Demnig, L. S.; Dening, W. S.; Teller, E. J Am Chem Soc 1940, 62, 1723.
31. Dubinin, M. M. Carbon 1998, 27, 457.
32. Laine, J.; Yunes, S. Carbon 1992, 30, 601.
33. Teng, H.; Wang, S. C. Carbon 2000, 38, 817.
34. Lin, C. C.; Teng, H. Ind Eng Chem Res 2002, 41, 1986.
35. Huang, M. C.; Teng, H. Carbon 2002, 40, 955.
36. Teng, H.; Yung, J. A.; Hsu, Y. F.; Hsieh, C. T. Ind Eng Chem Res 1996, 35, 4043.
37. Teng, H.; Ho, J. A.; Hsu, Y.-F. Carbon 1997, 35, 275.
38. Teng, H.; Yeh, T.-S. Ind Eng Chem Res 1998, 37, 58.
39. Patrick, J.-W. In Porosity in Carbon; Muhlen, H.-J.; Karl, H. Eds.; Edward Arnold: London, 1995; p 131.
40. Cai, Q. Huang, Z. H.; Kang, F.; Yang, J. B. Carbon 2004, 24, 775.